

Spatiotemporal dynamics in optically excited quantum wire-dot systems: Capture, escape, and wave-front dynamics

D. Reiter, M. Glanemann, V. M. Axt, and T. Kuhn

Institut für Festkörperteorie, Westfälische Wilhelms-Universität Münster, Wilhelm-Klemm-Str. 10, 48149 Münster, Germany

(Received 14 July 2006; revised manuscript received 17 November 2006; published 18 May 2007)

Transitions of optically excited carriers between delocalized states in a quantum wire and localized states in a quantum dot are studied on a quantum kinetic level. These transitions are mediated by the emission or absorption of longitudinal optical phonons. Three different excitation scenarios are considered: The capture of a traveling wave packet results in occupations of the bound states and, under suitable conditions, in coherent superpositions. Both occupations and coherences decay due to thermal escape processes resulting from the absorption of phonons. A spatially homogeneous excitation in the quantum wire below the threshold for optical phonon emission leads to capture processes associated with the buildup of a wave front in the carrier density between regions which are already influenced by the capture and regions where this influence is not yet present. A selective excitation of the quantum dot exciton is at elevated temperatures followed by thermal escape processes with a subsequent spreading of the carriers in the quantum wire. We find that for a physically meaningful description of the spatiotemporal dynamics a consistent treatment of both diagonal and off-diagonal density matrix elements is essential in all three scenarios.

DOI: [10.1103/PhysRevB.75.205327](https://doi.org/10.1103/PhysRevB.75.205327)

PACS number(s): 78.67.-n, 73.63.-b, 72.20.Jv, 72.10.Di

I. INTRODUCTION

In extended systems quantum mechanical scattering processes are intrinsically nonlocal in space. At the most basic level of theory this is due to the uncertainty between momentum and position. When, e.g., homogeneously distributed carriers interact with a phonon in an extended semiconductor we have a well-defined momentum transfer in the scattering process but even in principle no information about the position where the scattering takes place. For spatially inhomogeneous carrier distributions the quantum kinetic derivation of the scattering term for the Wigner function yields a spatial memory to comply with momentum-position uncertainty, in addition to the temporal memory which accounts for energy-time uncertainty.¹ The semiclassical Boltzmann scattering term is obtained from the quantum kinetic formula as the lowest order in a gradient expansion.² This, however, in general may violate the uncertainty relations. In samples that are spatially structured on a nanometer scale the local environment can have a profound impact on the scattering which then acquires a local character. This holds in particular for phonon-induced capture processes, where the carriers perform transitions between states of different effective dimensionality. The final state of a successful capture is more localized than the initial state and thus carries information where the scattering has taken place. In this case one should expect that a capture only takes place when the carrier is initially sufficiently close to the localized state and that regions far away should not be affected by the capture process. However, if the dynamics of such a system is described by kinetic equations for the occupations of the corresponding states, any capture process will instantaneously reduce the carrier density all over the structure. Analogously, the escape of a carrier from a localized state—e.g., by phonon absorption—will immediately populate the whole extended carrier state. Thus, in order to correctly describe the local character of capture and escape processes one has to go be-

yond a description in terms of occupations of the eigenstates.

There are many important examples for such capture processes, and calculations of the carrier dynamics have been performed on various levels of the theory. The trapping of carriers in the quasi-two-dimensional active region from three-dimensional transport states³⁻⁷ is a basic ingredient for a quantum well laser. Quantum dots are usually covered by a two-dimensional wetting layer, and thus carriers generated in the wetting layer may be scattered into zero-dimensional dot states.⁸⁻¹³ Also techniques have been developed to fabricate quantum wires with embedded quantum dots,¹⁴⁻¹⁶ either by cleaved edge overgrowth or by growth on a patterned substrate. Such structures support transitions between one-dimensional and zero-dimensional states.^{17,18} In the present paper we study phonon capture and escape processes induced by the interaction of the carriers with longitudinal optical (LO) phonons in quantum wire-dot systems. We show that spatial inhomogeneities that arise either from the spatial structure of the sample or from spatially focusing of the excitation lead to a pronounced local character of the scattering which is reflected in characteristic spatiotemporal signatures in the carrier dynamics. As we are dealing here with processes on short time and length scales, where the fundamental limitations set by the uncertainty relations should matter, a description along the lines of the semiclassical Boltzmann equation reaches its limits. Therefore, all calculations in the present paper are performed within the framework of a quantum kinetic theory.^{2,19,20}

Carrier capture processes of a localized traveling wave packet from a semiconductor quantum wire into a quantum dot at zero temperature have been studied in previous papers.^{17,18} There we have shown that the combination of ultrashort length and time scales gives rise to pronounced quantum mechanical features in the capture dynamics such as the appearance of phonon Rabi oscillations and the capture into superpositions of bound states.¹⁷ Both the occupations of the bound states and the quantum mechanical coher-

ences can be efficiently controlled by suitable two-pulse excitations.¹⁸ In the present paper we will first extend these studies involving a spatially localized excitation to higher temperature, where besides phonon emission also phonon absorption processes are possible. Due to these phonon absorption processes, carriers which have been trapped may be released again from the quantum dot.

Then we will address two other excitation scenarios: a delocalized, spatially homogeneous excitation of the quantum wire and a spectrally selective excitation of the quantum dot exciton. The central theme in these two scenarios will be the interplay between capture and escape processes and the spatiotemporal carrier dynamics in the quantum wire region. While for the modeling of the wave-packet dynamics mentioned above it is clear that off-diagonal density matrix elements are necessary to describe the localized carrier distributions generated by the focused light pulse, in the case of spatially homogeneous excitation this is less obvious. Here, the generation process essentially leads only to occupations of the states—i.e., to a diagonal density matrix. However, we will show that the local character of the capture and escape processes gives rise to off-diagonal density matrix elements and that a consistent treatment of diagonal and off-diagonal density matrix elements is crucial for a physically meaningful description of the spatiotemporal carrier dynamics.

As in our previous studies we focus on a quantum wire-dot structure as a prototype for structures involving electronic states with different effective dimensionality. However, we expect that in particular the dynamics after homogeneous excitation or after selective excitation of the quantum dot will be qualitatively similar in other structures like, e.g., a quantum dot in a quantum well or a quantum wire in a quantum well.

The paper is organized as follows: In Sec. II we briefly summarize the basic ideas of the theoretical approach. In Sec. III we show numerical results for three different scenarios. First we discuss the influence of the temperature on the capture of a traveling wave packet. In the second part we analyze the carrier dynamics and capture after a spatially homogeneous excitation in the quantum wire. In the last scenario we study the thermal escape of carriers generated in the quantum dot, which occurs at elevated temperatures. Finally, in Sec. IV we briefly summarize our results and draw some conclusions.

II. THEORY

In this paper we study on a quantum kinetic level the carrier dynamics in a semiconductor quantum wire with an embedded quantum dot. The semiconductor is described within a two-band model for electrons and holes. The quantum wire is of cylindrical shape and in the lateral directions confined by infinitely high potential barriers. In the longitudinal direction periodic boundary conditions are used. The quantum dot is shaped by a potential $V^{eh}(z) = -V_0^{e/h} \operatorname{sech}(z/a)$ for electrons and holes. While a describes the width of the potential, V_0^{eh} specifies the depth where V_0^e applies to the electrons and $V_0^h = \frac{2}{3}V_0^e$ to the holes. In this paper we consider a GaAs quantum wire with 100 nm² cross

section and different quantum dot parameters as specified below. Electron-hole pairs are generated in this structure by means of a short laser pulse. The laser pulse is coupled by the dipole interaction to interband transitions, and we will discuss both localized and delocalized excitations. The carriers are coupled to bulklike LO phonons with energy $\hbar\omega_{LO} = 36.4$ meV via the Fröhlich interaction. Bulklike, dispersionless phonon modes are indeed widely used and have provided good results.^{21–24} By including the Coulomb interaction on the mean-field level we furthermore account for excitonic effects.

The laser pulse is modeled by an electric field which is assumed to be Gaussian in time and space according to

$$\mathbf{E}^{(+)}(z, t) = \mathbf{E}_0 \exp\left(-\frac{t^2}{\tau^2} - \frac{(z - z_0)^2}{2\sigma_z^2} - i\omega t\right). \quad (1)$$

\mathbf{E}_0 describes the amplitude of the field, τ the pulse duration, and z_0 the position of the laser pulse with variance σ_z . The frequency $\omega = (\epsilon_{gap} + \Delta E)/\hbar$ corresponds to the mean excess energy ΔE above the band gap of the quantum wire ϵ_{gap} . By choosing σ_z much larger than the length of the structure this includes also the case of a spatially homogeneous excitation. We restrict ourselves to rather low excitation densities so we can treat the phonon system as a bath. At these low excitation densities the Coulomb interaction predominantly leads to excitonic and renormalization effects, which are fully described on the level of the mean-field approximation. We have taken care that the densities are low enough such that an excitation of multiexcitation states can be neglected.

The calculations are performed in the basis determined by the single-particle potentials for electrons and holes. As has been discussed in Ref. 17, in this representation the numerics is favorable for excitations near the band gap. The details of this model can be found in Refs. 1 and 17.

The basic dynamical variables in the density matrix approach to quantum kinetics are the single-particle density matrices defined as

$$\rho_{n',n}^e = \langle c_{n'}^\dagger c_n \rangle, \quad \rho_{n',n}^h = \langle d_n^\dagger d_{n'} \rangle, \quad p_{n',n} = \langle d_{n'} c_n \rangle, \quad (2)$$

where c_n^\dagger and d_n^\dagger (c_n and d_n) describe the creation (annihilation) of an electron and a hole in the n th eigenstate of the respective single-particle potential. The lowest few values of n correspond to the bound states in the quantum dot. The other values refer to the free states in the quantum wire, where the carriers can move along the z direction. The diagonal elements of the density matrix $\rho_{n,n}$ describe the occupations of the single-particle states. The off-diagonal elements $\rho_{n',n}$ ($n \neq n'$) of the density matrix describe the coherences between the states. The coherences include the information over the phase relations between the different states. In the discrete part they describe coherent superpositions which may show up as a result of the capture process. In the continuum part they carry the information on the spatial profile, e.g., of a wave packet generated by a localized excitation. Below we will study their role in the case of a spatially homogeneous excitation.

Because of the Coulomb and electron-phonon interactions, we are dealing with a many-body problem. Consequently, the equations of motion for the single-particle density matrices are not closed. They constitute the starting point of an infinite hierarchy of equations which for the electron-phonon interaction we truncate on the level of the quantum kinetic second Born approximation. The Coulomb interaction is treated on the mean-field level to account for excitonic effects and the Coulomb enhancement. The corresponding equations can be found in Refs. 1 and 17. In the next section we will analyze the ultrafast dynamics of optically excited carriers for different excitation scenarios and different temperatures.

III. RESULTS

A. Localized excitation in the quantum wire: Wave-packet capture at finite temperature

In the first case we excite the semiconductor with a laser pulse which has an excess energy of $\Delta E=20$ meV and a pulse duration of $\tau=50$ fs centered at $z_0=-90$ nm with $\sigma_z=10$ nm. Due to the symmetrical excitation in k space, the wave packet splits into two parts moving in opposite longitudinal directions of the quantum wire. Because the mass of the holes is much higher than the mass of the electrons, they move much slower and are therefore not of interest for the present discussion. Nevertheless, they are fully included in our calculation. When the electrons reach the quantum dot, they can be captured into the dot by the emission of an LO phonon. An extensive analysis of this capture process at zero temperature is given in Refs. 17 and 18. In this section we will extend these calculations to finite temperatures and study the influence of the temperature on the capture process.

For zero temperature there are no phonon absorption processes possible. Because the energy of the electrons is smaller than the LO phonon energy, also no phonon emission processes can occur while the electrons are in the quantum wire. Under these conditions the presence of the electron-phonon interaction is reflected only in polaronic dressing effects such as slight renormalizations of the electronic energies and of the effective mass. The phonon interaction is then effectively switched on only when the wave packet reaches the quantum dot.

Let us first consider a quantum dot with parameters $V_0^e=30$ meV and $a=4$ nm, which has a single bound level at $E=-14.4$ meV. Because the mean excess energy of the electrons is about one LO phonon energy above the energy of the dot state, the capture rate is maximal. The occupation of the bound state as a function of time is shown in Fig. 1 for different temperatures $T=0, 77, 150,$ and 300 K. For $T=0$ K we see a rise of the occupation up to 19% followed by a damped oscillation resulting in a final occupation of about 16% at $t=1.2$ ps. The oscillations reflect phonon Rabi oscillations between the bound state and the continuum states as discussed in detail in Ref. 17. For times longer than about 0.9 ps the occupation is approximately constant. At these times the coherent oscillations have decayed and, because of the absence of phonons, the trapped electrons cannot leave the dot anymore. For $T=77$ K the occupation does not differ

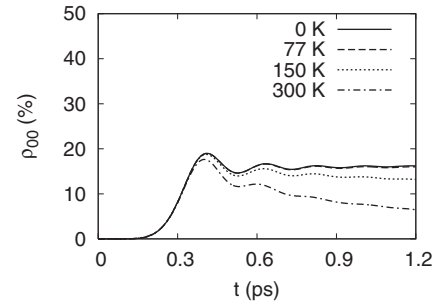


FIG. 1. Occupation of the quantum dot ground state after excitation of a traveling wave packet in the quantum wire for different temperatures. The quantum dot has a single bound state at -14.4 meV.

much from the $T=0$ K case at all times because at this temperature we still have $T \ll T_{LO} = \hbar \omega_{LO} / k_B = 423$ K. If we raise the temperature to $T=150$ K, the initial occupation still coincides with its low temperature value but a subsequent decay sets in which reduces the dot occupation to about 13% at $t=1.2$ ps. For room temperature $T=300$ K the decrease is much stronger and only 6% of the occupation is left in the quantum dot at $t=1.2$ ps. For higher temperatures an incoherent thermal emission of trapped electrons occurs, leading to a substantial decrease of the occupation. Electrons escape from the quantum dot by absorbing a phonon and can then travel in both directions away from the quantum dot. This incoherent escape process is in clear contrast to the coherent escape process associated with the phonon Rabi oscillations which occurs at short times. The Rabi oscillations lead to a directional emission of follow-up wave packets moving in the same direction as the initial wave packet. These wave packets are emitted always when the occupation of the bound state has a minimum—i.e., when the electronic density matrix has rotated back to the continuum states.¹⁷ We find that this coherent escape is present at all temperatures, but with increasing temperature the thermally activated incoherent escape eventually becomes dominant.

Let us now turn to a quantum dot with several bound levels. In this case the capture process may result not only in an occupation of the bound states but also in coherent superpositions of these states. As an example of a dot with three bound levels at -30.6 meV, -15.2 meV, and -5.8 meV ($V_0^e=40$ meV and $a=10$ nm) we discuss the influence of the temperature on the coherences. In Figs. 2(a) and 2(b) the occupations of the three bound levels as well as the total occupation of the bound states are shown for $T=0$ K and $T=300$ K, respectively. Figures 2(c) and 2(d) show the real part of the coherences between the bound levels for the two temperatures. All quantities have been normalized to the total number of generated electrons. In the zero-temperature case the total occupation rises up to more than 30% while at room temperature $T=300$ K the occupation reaches only 25% and decreases afterwards due to thermal escape processes. The coherences between the discrete dot states build up when the electrons reach the region of the dot and are oscillating in time with a period corresponding to the energy difference between the discrete dot states. While for $T=0$ K the oscillations are essentially undamped, for $T=300$ K we observe a clear damping of the oscillations.

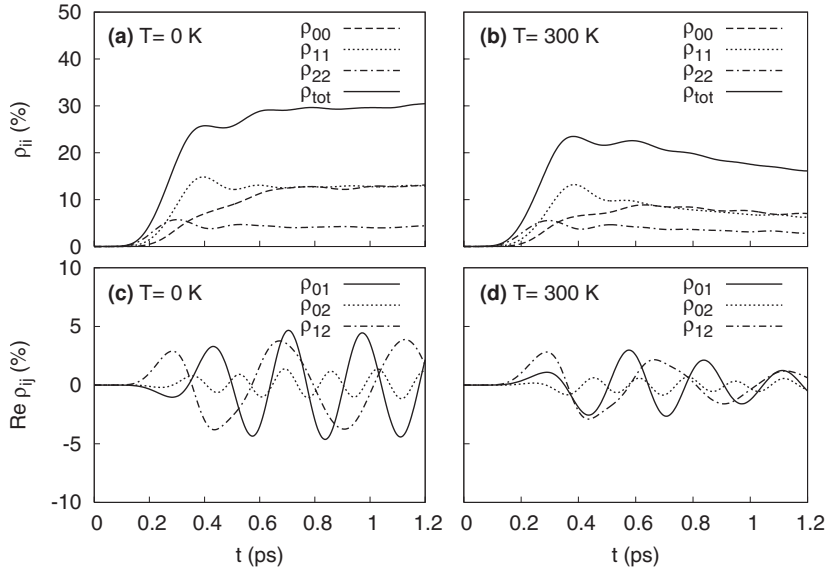


FIG. 2. Density matrix elements in the bound subspace of a quantum dot with three bound states after excitation of a traveling wave packet in the quantum wire. (a) and (b) Occupation of the ground state ρ_{00} and the first ρ_{11} and second ρ_{22} excited states for $T=0$ K and $T=300$ K, respectively; (c) and (d) real part of the coherences between the three discrete dot states for $T=0$ K and $T=300$ K.

For a quantitative analysis of this damping we have fitted the time dependence of the coherence between the two lowest bound states ρ_{01} by an exponentially damped sinusoidal oscillation. It turns out that this fit reproduces well the calculated curves after about 500 fs. The decay rates τ^{-1} obtained from this fit are shown for different temperatures as symbols in Fig. 3. Obviously we observe a strong increase with increasing temperature. It should be expected that this decay of the coherences, like in the case of the occupations, is a result of the thermal emission of the trapped electrons due to the absorption of phonons, which is proportional to the phonon occupation. The dashed curve in Fig. 3 shows the function

$$\tau^{-1} = \tau_0^{-1} \frac{1}{\exp\left(\frac{\hbar\omega_{LO}}{k_B T}\right) - 1}, \quad (3)$$

where the value of τ_0^{-1} has been obtained by a fit to the extracted decay rates and is given by $\tau_0^{-1} = 4.6$ ps $^{-1}$. Indeed, the temperature dependence of the decay rate is very well reproduced by the Bose function for LO phonons.

B. Delocalized excitation in the quantum wire: Capture and wave-front dynamics

After having analyzed the capture of a wave packet which has been generated by a strongly localized excitation, we

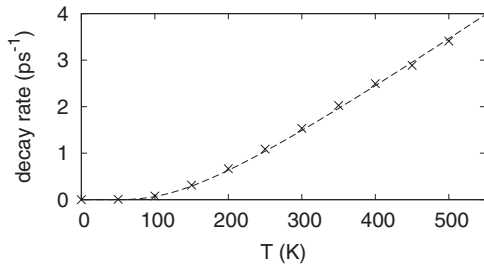


FIG. 3. Symbols: decay rate of the coherence ρ_{01} as a function of temperature extracted from the numerical data; line: fit to a Bose distribution of LO phonons.

will now address the carrier dynamics and capture processes after a spatially homogeneous excitation in the quantum wire. We again choose a laser pulse with a mean excess energy of 20 meV and a pulse duration of $\tau=50$ fs, but now the variance σ_z of the laser pulse is taken to be much larger than the length of the structure such that we achieve a spatially homogeneous excitation. Since coherences between the bound states are only created by spatially narrow wave packets,²⁵ such coherences will be of minor importance in the present case. Therefore we will limit ourselves to the quantum dot with a single bound level at -14.4 meV ($V_0^e = 30$ meV and $a=4$ nm). In order to avoid boundary effects a sufficiently large system size has to be taken. To keep the problem numerically tractable, in this scenario the Coulomb mean-field terms have been neglected. We have checked that, apart from some slight modification of the generated carrier density due to the missing Coulomb enhancement, this has essentially no influence on the carrier dynamics.

Figures 4(a) and 4(b) show the density of the free electrons—i.e., the density calculated without taking into account the bound state in the dot—at lattice temperatures of $T=0$ K and $T=300$ K, respectively, as a function of the spatial coordinate z for different times. At $t=0$ fs—i.e., at the pulse maximum—the density is indeed homogeneous outside the dot region. In the region of the quantum dot the density is reduced because of the orthogonality of the continuum states with respect to the bound state. At later times for both temperatures we observe on each side of the dot a wave front between a region with low density and a region with high density which moves at constant speed away from the dot. This wave front marks the transition between the regions where carriers at a given time are already missing due to the capture into the quantum dot from the region which is still unaffected by the capture. This interpretation is confirmed by looking at the corresponding Wigner function—i.e., the quantum analog to the classical distribution function—which is obtained by a suitable Weyl-Wigner transformation from the electron density matrix.¹ In contrast to the density profiles discussed above now also the bound state is included in the calculation of the Wigner function. This Wigner function

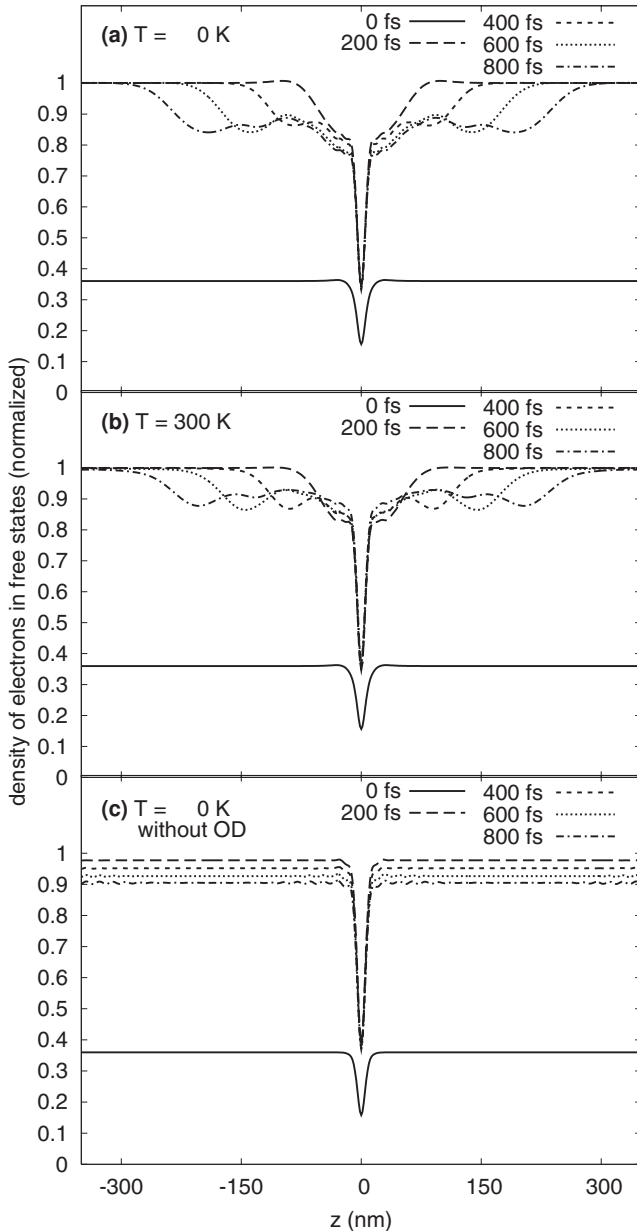


FIG. 4. Density of the free electrons as a function of the position after a spatially homogeneous excitation of the quantum wire with a 50-fs pulse (pulse maximum at $t=0$) at different times. (a) $T=0$ K, (b) $T=300$ K, and (c) $T=0$ K but without taking into account the off-diagonal elements of the density matrix.

is shown in Fig. 5 for two different times $t=0.2$ ps and $t=0.6$ ps at both temperatures. At $t=0.2$ ps, shortly after the excitation is finished, the Wigner function is essentially symmetric with respect to both space z and momentum k . The momentum distribution is determined by the spectral properties of the generating laser pulse and is concentrated around two maxima at $\pm k_{max}$ corresponding to the excess energy of 20 meV. At $t=0.6$ ps the captured density can be clearly observed at $z \approx 0$. Because of the spatial localization of the bound state the Wigner function extends to rather high k values around $z=0$. At the maxima of the momentum distribution at $\pm k_{max}$ two valleys have built up, for positive momenta in the positive z direction and for negative momenta in

the negative z direction, both beginning at $z=0$, where the dot is located. These valleys show up because the electrons are moving in the direction of their momenta. When reaching the dot those carriers which have an energy about one LO-phonon energy above the bound state are trapped inside the dot and therefore cannot pass the dot region. Thus, behind the dot these electrons are missing and a valley is formed in the momentum distribution. If the energy of the carriers does not satisfy the resonance condition for capture, the carriers pass the dot. These carriers are responsible for the lower plateau value in Figs. 4(a) and 4(b). The finite width of the valleys reflects the quantum kinetic energy-time uncertainty. A finite spread of phonon energies, which is neglected in the present paper, would further increase the width of the valleys, resulting in an additional spread of the velocity of the wave front and a reduction of the plateau value. For not too strong phonon dispersion we therefore expect only quantitative but no qualitative changes of the behavior predicted in this paper. Interestingly, not only the captured carriers but also the carriers which are not trapped because they are too far from the resonance condition for a capture process experience the presence of the dot which results in an increased group velocity around $z=0$. This leads to a slight structure in the Wigner function along the line $z=\hbar kt/m$.

As a further check of this interpretation we have performed calculations with a modified excess energy of the laser pulse of 10 meV instead of 20 meV before (not shown). Indeed we find again wave fronts in the density of free carriers moving away from the dot at the same speed as before. However, the plateau value of the density between these wave fronts is larger. This again demonstrates that the wave front results from carriers with an energy of $\hbar\omega_{LO}$ above the bound state. Therefore its speed depends only on the energy of the bound state. The excess energy determines the fraction of carriers which are available for a capture process and thus the total capture efficiency.¹⁸

The main features of the transport and capture dynamics discussed so far are the same for both temperatures 0 K and 300 K. This is because on the short length and time scales and for the excitation conditions chosen here the transport is to a large extent ballistic and therefore independent of temperature. However, when looking in detail differences between the two temperatures are clearly observable. First, the Wigner function for $T=300$ K exhibits nonzero values also at k values above the generated distribution. These are carriers which, after the optical generation, have absorbed a phonon. Second, when looking at the density of free carriers in the immediate vicinity of the dot we find that, while at zero temperature [Fig. 4(a)] this density is continuously decreasing with increasing time, at 300 K [Fig. 4(b)] it is increasing with time. Here we observe again the thermal escape of carriers which previously have been trapped. Like in the case of the traveling wave packets discussed above, this thermal escape leads to a reduced occupation of the bound state as is shown in Fig. 6 where the ground-state occupation is plotted as a function of time for $T=0$ K (solid line) and $T=300$ K (dashed line). While the zero-temperature curve exhibits a linear growth in the full time range shown, the 300-K curve bends down and leads to an occupation which is at $t=1.2$ ps only about 50% of the corresponding low-temperature value.

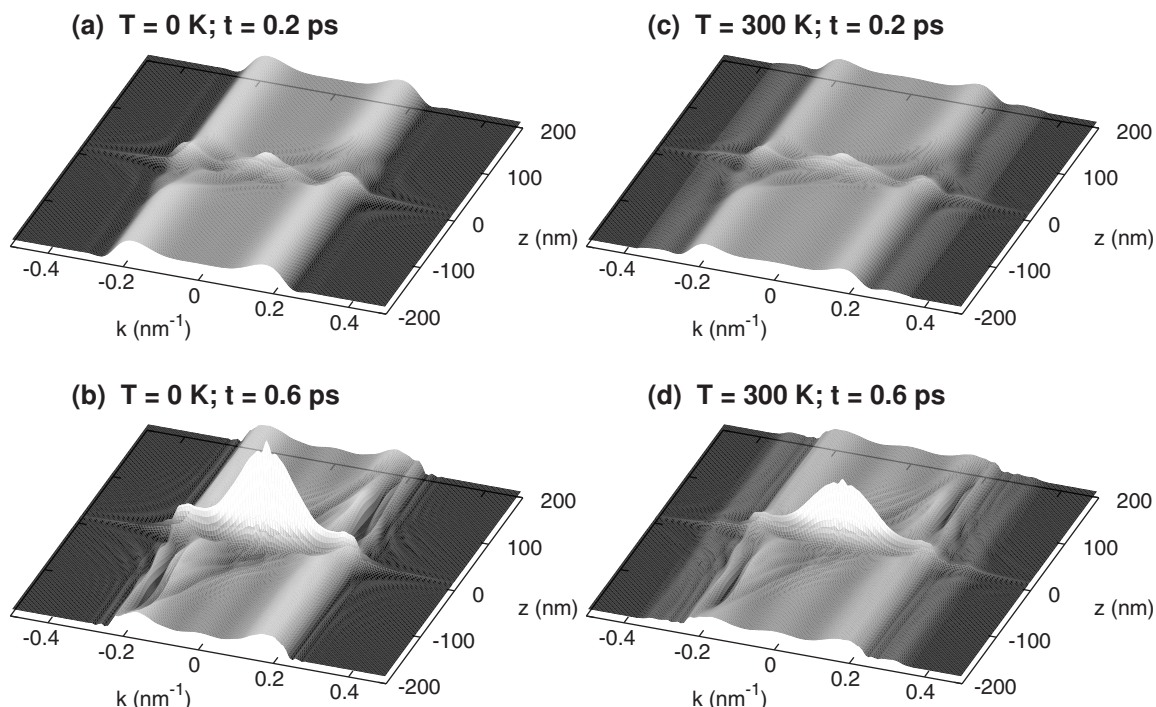


FIG. 5. Wigner function of the electrons after a spatially homogeneous excitation of the quantum wire with a 50-fs pulse (pulse maximum at $t=0$) for the temperatures $T=0$ K [(a),(b)] and $T=300$ K [(c),(d)] at times $t=0.2$ ps [(a),(c)] and $t=0.6$ ps [(b),(d)].

In the case of a spatially homogeneous excitation the carrier generation leads to an essentially diagonal electron density matrix; i.e., the eigenstates of the single-particle potential are occupied with a certain probability but there is nearly no coherence between different eigenstates. When modeling the carrier capture by semiclassical capture rates¹⁰ but also in quantum kinetic calculations¹² it is then often assumed that off-diagonal elements can be neglected in the carrier dynamics. In order to analyze the role of off-diagonal electron density matrix elements in our scenario we have performed calculations where we have switched off all these off-diagonal elements. The resulting density profiles at different times for $T=0$ K are shown in Fig. 4(c). Obviously, the spatiotemporal dynamics of the electrons in the wire region is completely different when off-diagonal elements are neglected. Without off-diagonal elements no spatially inhomogeneous profiles

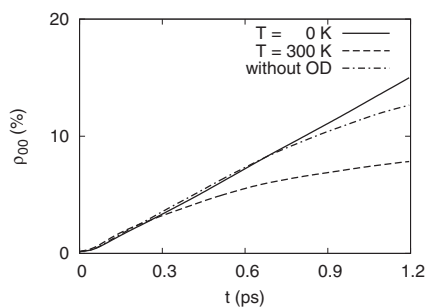


FIG. 6. Occupation of the quantum dot ground state after a spatially homogeneous excitation of the quantum wire with a 50-fs pulse (pulse maximum at $t=0$). Solid line: $T=0$ K. Dashed line: $T=300$ K. Dash-dotted line: $T=0$ K but without taking into account the off-diagonal elements of the density matrix.

can be present. Therefore, the capture process reduces the density in the free states simultaneously in the whole system. This is in sharp contrast to the picture of a local capture process which should result in a trapping of only those carriers which are close to the dot. This local picture is clearly supported by the full calculation including off-diagonal elements. The different dynamical behavior in the wire region also modifies the occupation of the bound state, as can be seen in Fig. 6 (dash-dotted line). As already mentioned, in the full calculation at $T=0$ K the occupation grows linearly over the whole time interval shown. The reason is that the wave fronts in Fig. 4(a) have not yet reached the boundary of the system. Therefore, the distribution of carriers arriving at the dot is not yet affected by previous capture processes and thus, since the excitation density has been chosen sufficiently weak such that phase-space-filling effects of the final state are negligible, the effective capture rate is constant over the whole time interval. In contrast, when neglecting the off-diagonal elements of the density matrix we observe a clear deviation from the linear growth of the ground-state occupation. As is evident from Fig. 4(c), since the density of free carriers is reduced in the whole structure, the finite system size may influence the capture dynamics from the beginning. The reduction of the carriers which are available for the trapping process then reduces the effective capture rate, leading to a bending of the corresponding curve in Fig. 6.

C. Excitation of the quantum dot: Thermal escape processes

In the previous sections we have seen that at higher temperatures a thermal escape of electrons from the bound states to the continuum states occurs, leading to a reduction of the effective capture rate and a decrease of both occupations and

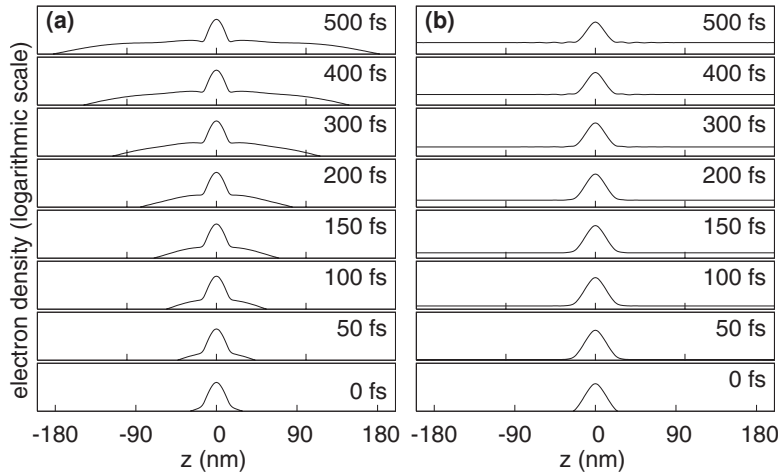


FIG. 7. Electron density as a function of position on a logarithmic scale at different times after selective excitation of the quantum dot ground state exciton by a 200-fs laser pulse. The temperature is $T=300$ K. (a) Full model including the off-diagonal density matrix elements and (b) without the off-diagonal elements.

coherences after the capture has finished. Let us now concentrate on this thermal escape process by choosing an optical excitation with an excess energy $\Delta E = -52$ meV corresponding to the lowest quantum dot exciton state of the structure with a single-electron bound state at -14.4 meV. The pulse duration is $\tau = 200$ fs, such that only the ground-state quantum dot exciton is excited. The excitation is taken to be spatially homogeneous; however, in the present case this is less important since only the overlap of the light field with the quantum dot exciton is relevant. At zero temperature, except for some very small effects resulting from the polaron dressing process, the electron and hole density matrices are essentially constant after the excitation process. Therefore, in the following we will concentrate on the case of $T=300$ K.

The dynamics of the escape process is presented in Fig. 7(a) which shows the spatially resolved electronic density in real space on a logarithmic scale. At $t=0$ fs we see the peak of the bound density inside the quantum dot at $z=0$, where the ground state of the quantum dot was excited and no density in the region of the quantum wire outside the dot. With increasing time we find electrons at both sides of the dot which are traveling away from it. These electrons have escaped from the quantum dot by absorbing a phonon. We can see a constant outflow from the quantum dot and an electron density extending over an increasingly large region of the structure. The spatiotemporal behavior of the holes is similar to that one of the electrons, but the holes move much slower because of their higher mass (not shown).

This incoherent escape manifests itself in a symmetrical outflow of the electrons at both sides of the dot. This is in contrast to the coherent escape associated with phonon Rabi oscillations induced by the capture of a traveling wave packet, where wave packets are emitted only in the direction of the incoming wave packet.¹⁷ The Rabi oscillations occur between the initial (free) state of the electron without phonon and the final (trapped) state with the emitted phonon. When one Rabi cycle is completed, the electrons are back in the initial state and have a certain probability to leave the dot region. However, the initial state has a certain direction given by the direction of the incoming wave packet which therefore determines the direction of the emitted wave packets.

The occupation of the ground state for the electrons is shown in Fig. 8 (solid line). The occupation is normalized to

the total occupation of all states, which remains constant after the pulse has finished. During the generation process we see the occupation rising monotonically and it reaches a maximum of about 80% at about 250 fs. The fact that this value is considerably below 100% shows that thermal escape is rather efficient already during carrier generation. Later on the bound-state occupation decreases monotonically due to the thermal escape processes and the carriers move away from the dot as discussed above.

These results obtained from the full quantum kinetic calculation with all elements of the density matrix are now again compared to calculations where the off-diagonal elements have been neglected. The resulting profiles of the carrier density (on a logarithmic scale) are shown in Fig. 7(b), and the occupation of the electron ground state is plotted as dashed line in Fig. 8. As in the previous section we find again that the spatiotemporal dynamics cannot be reproduced without taking into account the off-diagonal elements. With this approximation the escape of a carrier from the bound state due to phonon absorption immediately results in an occupation in the whole system which is in clear contrast to the local nature of carrier-phonon interaction. Also when looking at the occupation of the bound state (Fig. 8) we observe pronounced differences. After the initial rise due to the carrier generation process, the dashed line decays much faster than the solid line and after about 1 ps it reaches a steady state. This can again be understood from the fact that

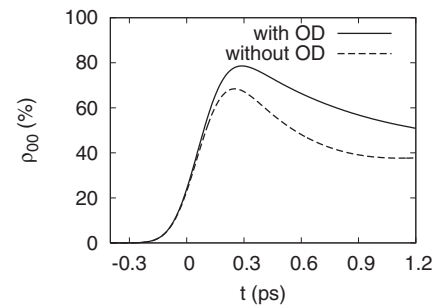


FIG. 8. Occupation of the quantum dot ground state after selective excitation of the quantum dot ground-state exciton by a 200-fs laser pulse. The temperature is $T=300$ K. Solid curve: full model including the off-diagonal density matrix elements. Dashed curve: without the off-diagonal elements.

without off-diagonal density matrix elements the thermal escape populates states in the whole structure. We then have a dynamical behavior which is similar to that one described by simple rate equations for the occupations of the states: After an initial evolution on a time scale determined by the inverse transition rates a steady state is reached where phonon absorption and emission processes balance each other. This time scale is here of the order of a few hundred femtoseconds. In contrast, in the full calculation no steady state can be reached before the carriers in the continuum states have reached the boundary of the system.

IV. CONCLUSIONS

In this paper we have analyzed the spatiotemporal dynamics of optically excited carriers associated with transitions between states of different dimensionality. To be specific, we have studied a quantum wire with an embedded quantum dot where transitions between the states occur due to the emission or absorption of LO phonons. The main subjects of our present analysis have been the role of the temperature and the dynamics of a wave front resulting from a combination of local capture and escape processes with the essentially ballistic motion of carriers with energies below the LO phonon energy in the quantum wire region.

In the case of the capture of a traveling wave packet, which has been studied previously at $T=0$ K, we find that finite temperatures lead to a decay of the occupations of the bound quantum states as well as of the coherences among these states. This decay is due to phonon absorption processes leading to a thermal emission of carriers which have been trapped previously. Indeed, the temperature dependence of the decay rates is well described by the equilibrium Bose distribution of the LO phonons. In contrast to the coherent escape associated with phonon Rabi oscillations, which leads to the emission of follow-up wave packets traveling in the same direction as the incident wave packet, the thermal escape occurs symmetrically into both directions.

When the carriers are generated spatially homogeneously in the quantum wire, the capture process leads to the build up of wave fronts in the carrier density profile between the regions which are already influenced by the carrier capture and those which have not yet experienced this influence. The wave fronts move at a velocity given by the group velocity of carriers which are one LO phonon energy above the bound state, because these carriers are most efficiently captured. The plateau value of the density between the wave fronts, on the other hand, is determined by the excess energy of the

exciting laser pulse, because this excess energy determines the total capture efficiency. For an accurate description of this spatiotemporal dynamics it is important to include off-diagonal density matrix elements of the carrier density matrices even in the case of a homogeneous excitation, since they contain the information on spatial inhomogeneities arising from the combination of transport and capture.

Finally we have studied the thermal escape process after selective excitation of the lowest quantum dot exciton state. The thermal escape leads to a characteristic spatiotemporal dynamics of the ejected carriers in the quantum wire which move ballistically away from the quantum dot. In this case again a neglect of the off-diagonal elements leads to an unphysical behavior in the description of this dynamics. But also the dynamics of the occupation of the bound states exhibits pronounced differences when comparing calculations with and without off-diagonal elements. Without off-diagonal elements a steady state is reached much earlier, because the ejected carriers immediately notice the finite system size while in the full calculation they have to reach the boundary by transport.

A possible scheme in order to monitor the quantum dot occupation relevant for the capture or escape scenario could be a spectrally and temporally resolved pump-probe experiment resonant on the quantum dot level. To observe the spatiotemporal carrier wave front dynamics in the quantum wire region a sufficiently high spatial resolution is required. This might be achieved with near-field techniques,^{26,27} for which spatial resolutions of a few nanometers have already been demonstrated.²⁸

In summary, we have shown that a quantum kinetic treatment of the interacting carrier-phonon system provides a consistent description of the ultrafast light-induced dynamics in structures involving states of different dimensionality both for localized and delocalized optical excitation. It avoids the necessity of preselecting the final state of a scattering process which is necessary when calculating a semiclassical rate according to Fermi's golden rule and therefore is able to describe the capture into superposition states. Furthermore, by including the off-diagonal elements of the density matrix, transport and scattering processes are treated on the same footing and all the fundamental uncertainty relations such as the uncertainties between time and energy or between position and momentum are fully accounted for. The full calculations clearly reveal the local character of phonon-induced capture and escape processes by affecting only the continuum occupations in the vicinity of the quantum dot.

¹M. Herbst, M. Glanemann, V. M. Axt, and T. Kuhn, *Phys. Rev. B* **67**, 195305 (2003).

²H. Haug and A.-P. Jauho, *Quantum Kinetics in Transport and Optics of Semiconductors* (Springer, Berlin, 1998).

³H. Shichijo, R. M. Kolbas, N. Holonyak, R. D. Dupuis, and P. D. Dapkus, *Solid State Commun.* **27**, 1029 (1978).

⁴J. A. Brum and G. Bastard, *Phys. Rev. B* **33**, 1420 (1986).

⁵T. Kuhn and G. Mahler, *Solid-State Electron.* **32**, 1851 (1989).

⁶P. W. M. Blom, C. Smit, J. E. M. Haverkort, and J. H. Wolter, *Phys. Rev. B* **47**, 2072 (1993).

⁷M. Preisel and J. Mørk, *J. Appl. Phys.* **76**, 1691 (1994).

⁸R. Ferreira and G. Bastard, *Appl. Phys. Lett.* **74**, 2818 (1999).

- ⁹I. Magnusdottir, S. Bischoff, A. V. Uskov, and J. Mørk, *Phys. Rev. B* **67**, 205326 (2003).
- ¹⁰A. Markus and A. Fiore, *Phys. Status Solidi A* **201**, 338 (2004).
- ¹¹T. R. Nielsen, P. Gartner, and F. Jahnke, *Phys. Rev. B* **69**, 235314 (2004).
- ¹²J. Seebeck, T. R. Nielsen, P. Gartner, and F. Jahnke, *Phys. Rev. B* **71**, 125327 (2005).
- ¹³S. Trumm, M. Wesseli, H. J. Krenner, D. Schuh, M. Bichler, J. J. Finley, and M. Betz, *Appl. Phys. Lett.* **87**, 153113 (2005).
- ¹⁴G. Schedelbeck, W. Wegscheider, M. Bichler, and G. Abstreiter, *Science* **278**, 1792 (1997).
- ¹⁵C. Lienau, V. Emiliani, T. Guenther, F. Intonti, T. Elsaesser, R. Nötzel, and K. H. Ploog, *Phys. Status Solidi A* **178**, 471 (2000).
- ¹⁶W. Wegscheider, G. Schedelbeck, G. Abstreiter, M. Rother, and M. Bichler, *Phys. Rev. Lett.* **79**, 1917 (1997).
- ¹⁷M. Glanemann, V. M. Axt, and T. Kuhn, *Phys. Rev. B* **72**, 045354 (2005).
- ¹⁸D. Reiter, M. Glanemann, V. M. Axt, and T. Kuhn, *Phys. Rev. B* **73**, 125334 (2006).
- ¹⁹V. M. Axt and T. Kuhn, *Rep. Prog. Phys.* **67**, 433 (2004).
- ²⁰F. Rossi and T. Kuhn, *Rev. Mod. Phys.* **74**, 895 (2002).
- ²¹S. Hameau, Y. Guldner, O. Verzelen, R. Ferreira, G. Bastard, J. Zeman, A. Lemaître, and J. M. Gérard, *Phys. Rev. Lett.* **83**, 4152 (1999).
- ²²O. Verzelen, R. Ferreira, and G. Bastard, *Phys. Rev. Lett.* **88**, 146803 (2002).
- ²³E. A. Zibik, L. R. Wilson, R. P. Green, G. Bastard, R. Ferreira, P. J. Phillips, D. A. Carder, J-P. R. Wells, J. W. Cockburn, M. S. Skolnick, M. J. Steer, and M. Hopkinson, *Phys. Rev. B* **70**, 161305(R) (2004).
- ²⁴P. Gartner, J. Seebeck, and F. Jahnke, *Phys. Rev. B* **73**, 115307 (2006).
- ²⁵M. Glanemann, V. M. Axt, and T. Kuhn, *Phys. Status Solidi C* **0**, 1523 (2003).
- ²⁶T. Guenther, C. Lienau, T. Elsaesser, M. Glanemann, V. M. Axt, T. Kuhn, S. Eshlaghi, and A. D. Wieck, *Phys. Rev. Lett.* **89**, 057401 (2002).
- ²⁷T. Unold, K. Mueller, C. Lienau, T. Elsaesser, and A. D. Wieck, *Phys. Rev. Lett.* **94**, 137404 (2005).
- ²⁸J. M. Gerton, L. A. Wade, G. A. Lessard, Z. Ma, and S. R. Quake, *Phys. Rev. Lett.* **93**, 180801 (2004).